Chemistry & Biology
Article

Arabidopsis P-Glycoprotein19 Participates in the Inhibition of Gravitropism by Gravacin

Marcela Rojas-Pierce,[1,2] Boosaree Titapiwatanakun,[3] Eun Ju Sohn,[1,2] Fang Fang,[4] Cynthia K. Larive,[4] Joshua Blakeslee,[3] Yan Cheng,[3] Sean Cuttler,[1,2] Wendy A. Peer,[3] Angus S. Murphy,[3] and Natasha V. Raikhel[1,2,*]
[1]Department of Botany and Plant Sciences
[2]Center for Plant Cell Biology
University of California, Riverside, Riverside, CA 92521, USA
[3]Department of Horticulture, Purdue University, West Lafayette, IN 47907, USA
[4]Chemistry Department, University of California, Riverside, Riverside, CA 92521, USA
*Correspondence: nraikhel@ucr.edu
DOI 10.1016/j.chembiol.2007.10.014

SUMMARY

ATP-binding cassette (ABC) transporters have been implicated in a multitude of biological pathways. In plants, some ABC transporters are involved in the polar transport of the plant hormone auxin and the gravitropic response. We previously identified Gravacin as a potent inhibitor of gravitropism in *Arabidopsis thaliana*. We demonstrate that P-glycoprotein19 (PGP19) is a target for Gravacin and participates in its inhibition of gravitropism. Gravacin inhibited the auxin transport activity of PGP19 and PGP19-PIN complexes. Furthermore, we identified E1174 as an important residue for PGP19 activity and its ability to form active transport complexes with PIN1. Gravacin is an auxin transport inhibitor that inhibits PGPs, particularly PGP19, which can be used to further dissect the role of PGP19 without the inhibition of other auxin transporters, namely PIN proteins.

INTRODUCTION

ATP-binding cassette (ABC) transporters comprise one of the largest families of proteins in most organisms, are mostly membrane associated, and couple ATP hydrolysis to the transport of a multitude of compounds across biological membranes. In eukaryotes, ABC transporters have been implicated in the transport of ions, sugars, peptides, and xenobiotics [1]. The founding ABC transporter, human multidrug resistance/P-glycoprotein (MDR1/P-gp), and other ABC transporters have been implicated in multidrug resistance in cancer and the development of several diseases such as cystic fibrosis [2]. In plants, ABC transporters translocate a diverse array of molecules including the plant hormone auxin, lipids, xenobiotics, and secondary metabolites (reviewed in [3]). *Arabidopsis* P-glycoprotein PGP19 (PGP19/MDR1/ABCB19) and PGP1 belong to the ABC type B transporter/multidrug resistance/P-glycoprotein family of proteins (TC 3.A.1) [4, 5] and together with the PIN-FORMED (PIN) family of proteins have auxin efflux activity [6–9]. PIN proteins are transmembrane proteins that belong to the auxin efflux carrier family (TC 2.A.69) [10, 11], and primarily regulate the basal levels of directional auxin transport required for polar development [10, 12, 13]. PGP19 and PGP1 were isolated from detergent-resistant microdomains (DRMs) of *Arabidopsis* microsomal fractions that bind the polar auxin transport inhibitor naphthylphthalamic acid (NPA) [14, 15]. Analysis of *pgp19* and *pgp1* mutants indicated that PGP19 and PGP1 function as auxin transporters in shoots and roots [15–17]. PGP19 has been shown to function primarily in basipetal transport along the embryonic shoot to root apical axis [16, 18–20] with an additional localized role in movement of auxin in the lateral root cap cells above the columella and below the elongation zone [7, 20]. Loss of *PGP19* function results in eccentric linear root growth, but has no effect in short-term root gravitropism [19]. PGP19 is localized to the shoot apex and the vascular tissues in light-grown hypocotyls, and its expression is upregulated throughout most of the hypocotyl in dark-grown seedlings [20]. In roots, PGP19 expression and abundance in cells involved in differential auxin movement in gravitropic responses are low or not detectable [7, 18, 20].

Auxin is synthesized at the shoot apex as well as in leaf and root primordia [21]. Auxin from the shoot apex is loaded into a stream of basipetal auxin flow along the embryonic axis that reaches the root tip via the vascular cylinder. Because auxin influx can occur by passive uptake, directional auxin flow is defined primarily by the polar activity of efflux carriers [19–22], except at the root tip, where the AUX1 H^+ auxin uptake symporter is involved [23, 24]. PIN and PGP proteins appear to act as independent auxin efflux carriers and are sensitive to auxin transport inhibitors, but they show reduced substrate and inhibitor specificity when expressed alone in nonplant heterologous systems [9]. The synergistic interaction of PIN and PGP proteins may provide the specificity and high rate of auxin transport necessary to generate a long-distance transport stream [19]. This model is supported by genetic interactions between PIN and PGPs and by coimmunoprecipitation and yeast two-hybrid assays.

Coexpression of PIN1 with PGP19 or PGP1 in HeLa cells results in a synergistic effect on auxin transport quantity and specificity in this system [20].

Plants respond to changes in gravitropic stimuli to ensure access to resources after strong winds or heavy rain. Sedimentation of starch-filled amyloplasts (statoliths) in gravistimulated columella cells of the root cap or the endodermis of hypocotyls triggers organ bending to align the plant axis with the gravity vector [25]. The plant auxin indole acetic acid (IAA) is the primary hormonal signal that regulates organ curvature by inducing differential growth between the upper and lower parts of gravistimulated tissues. Soon after gravistimulation, a gradient of auxin accumulation is formed between upper and lower parts of roots and hypocotyls [26–29], and differential polar auxin transport streams are required for this effect. In shoots, increased endogenous auxin levels promote cellular elongation, whereas in roots, localized differential auxin accumulations in the elongation zone inhibit elongation growth.

The precise mechanisms involved in lateral redistribution of auxin in gravistimulated tissues are still poorly understood. As auxin is a weak acid and its transport is motivated by chemiosmotic potentials, rapid differential activation of plasma membrane H^+ ATPases may contribute to lateral redirection [30]. In roots, redirection of auxin flows appears to be partially controlled by dynamic relocalization of PIN3 as well as internalization and proteolysis of PIN2 [31–33]. Less is known about the mechanisms of lateral auxin redirection in graviresponding hypocotyls. Tropic bending in hypocotyls may also involve PIN3 [33], and lateral auxin redistribution may involve interruption of PIN1- and PGP19-mediated downward auxin transport, especially as loss of *PGP19* function enhances tropic bending [20, 34, 35].

We recently identified 3-(5-[3,4-dichlorophenyl]-2-furyl)-acrylic acid (PubChem compound ID 776105, ChemBridge ID 5850247, herein referred to as Gravacin for *gra*vitropism and *vac*uolar transport *in*hibitor) as a strong inhibitor of root and shoot gravitropism, auxin responsiveness, and protein trafficking to the tonoplast in *Arabidopsis* [36]. Here we describe the identification of PGP19 as a target of Gravacin. We show that mutations in *PGP19* confer resistance to the effect of Gravacin on hypocotyl gravitropism and result in reduced binding of Gravacin to microsomal fractions. Gravacin was found to be a strong inhibitor of PGP19-mediated polar auxin transport in *Arabidopsis* and HeLa cells.

RESULTS

Gravacin Inhibits Gravitropism and Protein Trafficking via Independent Mechanisms

We initially identified Gravacin by screening a combinatorial library for effects on the gravitropic response of *Arabidopsis* seedlings [36]. Gravacin strongly inhibited gravitropism and blocked the trafficking of the tonoplast marker GFP-δTIP to the vacuolar membrane [36]. Thus, the GFP-δTIP marker displays a pattern similar to that of markers for the endoplasmic reticulum (ER) when seedlings are grown in the presence of Gravacin [36]. We tested the effect of eight compounds that were structurally similar to Gravacin (SciFinder Scholar, American Chemical Society) to understand the activity of Gravacin in these two pathways (Table 1). The effect of these compounds on gravitropism was assayed by quantification of the hypocotyl curvature in gravistimulated seedlings in the presence of 0.1, 1, or 10 μM each compound. Only Gravacin and compound A had strong inhibitory effects on gravitropism, and 1 μM was sufficient to inhibit the gravitropic response in hypocotyls (Table 1). The effect of these compounds on the trafficking of the GFP-δTIP marker was tested at 0, 2.5, 5, 10, and 35 μM. A minimum of 10 μM Gravacin was necessary to induce the ER-like appearance of the GFP-δTIP marker. In contrast, only 2.5 μM was needed to induce a similar phenotype with compounds C, D, E, and G, and 5 and 10 μM compounds A and F, respectively. However, compound B required 35 μM to induce this phenotype. Out of the eight compounds tested overall, only Gravacin and compound A were effective inhibitors of both pathways. We conclude that the chemical domains of Gravacin and its analogs that are required for inhibition of gravitropism and tonoplast protein trafficking are different, and independent targets must be responsible for the effects in each pathway.

Screen for Gravacin-Resistant Mutants

In order to identify the target of Gravacin responsible for the gravitropic phenotype, we conducted a genetic screen for mutants resistant to this effect. About 220,000 seeds from M_2 mutagenized plants in the GFP-δTIP background [37] were screened in a gravitropic assay for resistance to 1.7 μM Gravacin, a concentration that inhibits the gravitropic response of *Arabidopsis* hypocotyls [36] (Figure 1A). Seven resistant lines that were responsive to gravitropism in the presence of Gravacin were identified but only three lines showed strong resistant phenotypes, and were named Gra*vacin-resistant for gravitropism* (*grav-r*) (Figure 1A). Treatment of GFP-δTIP seedlings with 1.3 μM Gravacin resulted in a random distribution of hypocotyl orientations even 24 hr after a 90° reorientation, which indicates a strong inhibition of the gravitropic response (Figure 1B). In contrast, the orientations for over 60% of the GFP-δTIP hypocotyls in the DMSO control were 30°–90° from the gravity vector prior to reorientation. The *grav-r1* line is resistant to Gravacin, as over 90% of seedlings displayed hypocotyl curvatures between 30° and 90° in the Gravacin treatment (Figure 1B). Analysis of seedling extracts ruled out the possibility that the resistant phenotype of *grav-r1* was due to reduced uptake or abnormal metabolism of Gravacin (see the Supplemental Data available with this article online), and this line was selected for further characterization.

The *grav-r1* Mutation Maps to the *PGP19* Locus

A map-based cloning approach was used to identify the mutation in *grav-r1*. Forty-nine resistant mutants were identified in a mapping population of 301 F_2 segregating seedlings (1:6.14) using the gravitropic assay indicating

Table 1. Activity of Gravacin Analogs on Gravitropism and the Targeting of the GFP-δTIP Marker

Name	PubChem CID Numbers	Chemical Structures	Gravitropism (μM)	GFP-δTIP Targeting (μM)
Gravacin	776105	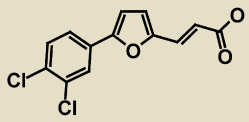	1	10
A	744897	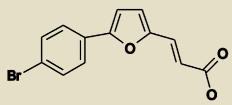	1	5
B	876446	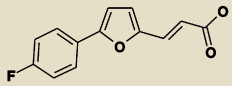	N/A	35
C	1106183	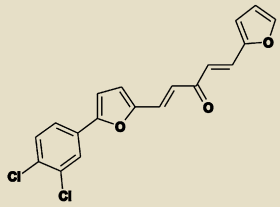	N/A	2.5
D	643402	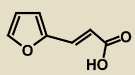	N/A	2.5
E	617688	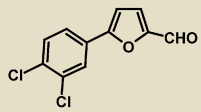	N/A	2.5
F	931655	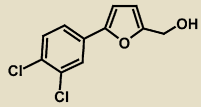	N/A	10
G	736257	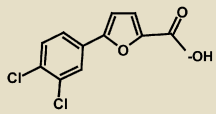	N/A	2.5

Compound identification (CID) numbers from PubChem are indicated. The numbers represent the minimum concentration at which an inhibitory effect was detected for each phenotype. Effect on hypocotyl gravitropism was tested at 0.1, 1, and 10 μM. GFP-δTIP targeting was tested at 0, 2.5, 5, 10, and 35 μM each chemical. N/A, no effect detected.

that the phenotype was due to a single recessive mutation. Rough mapping with SSLP markers [38] placed the mutation in chromosome 3 between markers ciw11 and ciw4. Fine mapping defined an interval of 639 kb containing the mutation between markers GL1 and MASC1094. This region contained the candidate gene *P-GLYCOPROTEIN* (*PGP*) *19*, a multidrug resistance ABC transporter that has been implicated in auxin efflux [15]. This gene was sequenced in the *grav-r1* mutant and a G to A substitution was found in the last exon of the gene, 6761 bp downstream of the start codon in the genomic sequence (Figure 1C). This results in a substitution of Glu1174 for Lys (E1174K) at a position adjacent to the predicted Walker B motif of the ATP-binding cassette of this protein (VLLLD*E*). We named this allele *pgp19-4* (Figure 1C).

To determine whether the mutation in *PGP19* was responsible for the Gravacin-resistant phenotype of *pgp19-4*, three other mutant alleles, *pgp19-1* (also known as *pgp19* or *mdr1-1*) [15], *mdr1-100*, and *mdr1-101* [39] (Figure 1C) were tested in the gravitropic assay in the presence of Gravacin. These knockout alleles display

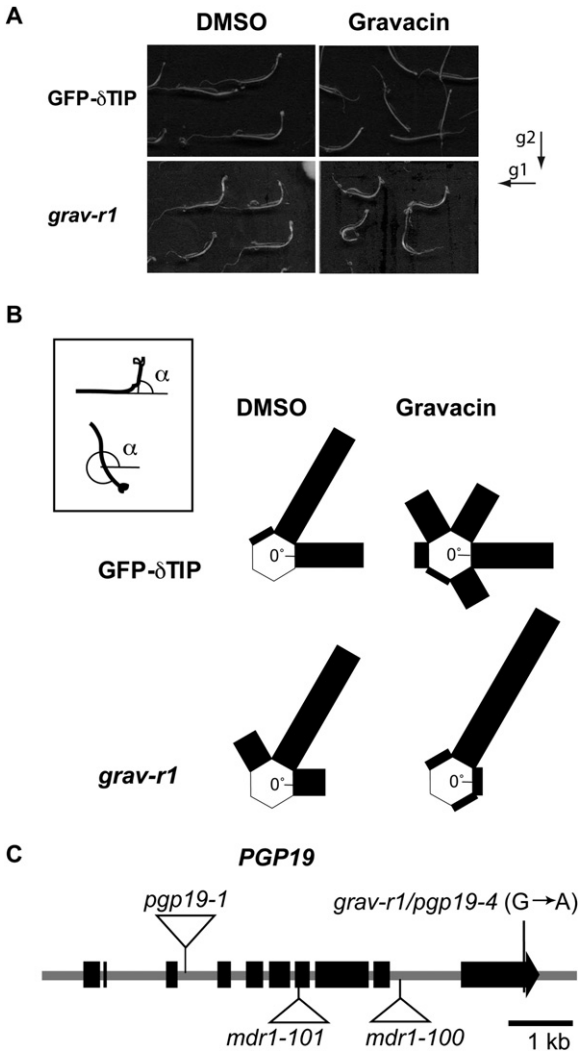

Figure 1. *gravacin-r1* Mutants Are Resistant to the Gravitropic Inhibition of Gravacin

(A) Gravacin inhibits gravitropic response of hypocotyls from the parental line (GFP-δTIP) but not of the *gravacin-r1* (*grav-r1*) mutant. Seeds from the GFP-δTIP parental line (top) and *grav-r1* mutant (bottom) were plated in the presence of DMSO (control, left) or 1.3 μM Gravacin (right) and 3-day-old seedlings were gravistimulated in the dark for 24 hr. Gravitropic vectors before (g1) and after (g2) reorientation are indicated.

(B) Quantification of the gravitropic response of the parental line (GFP-δTIP) and the *grav-r1* mutant. The experiment was done exactly as in (A). The angle formed between the upper hypocotyl of each seedling and the gravitropic vector before reorientation (g1) was measured and assigned to one of six 60° sectors (330°–30°, 30°–90°, 90°–150°, 150°–210°, 210°–270°, or 270°–330°). The small inset shows examples of the angle (α) used to measure hypocotyl orientation. Results are presented as the percentage of seedlings in each sector (n = 70–100 seedlings).

(C) The *grav-r1/pgp19-4* mutant line carries a G→A substitution in exon X of the *pgp19* coding sequence, 6761 bp downstream of the start codon. The T-DNA insertions in *pgp19-1*, *mdr1-100*, and *mdr1-101* are indicated.

enhanced hypocotyl gravitropism under normal conditions [34, 39]. Gravacin strongly inhibited the gravitropic response of the wild-type control Wassilewskija (Ws) but not that of the *pgp19-1* mutants (Figure 2), indicating that *pgp19-1* is also resistant to Gravacin. Similarly, *mdr1-100* and *mdr1-101* were also resistant to Gravacin (Figure S2). In comparison, a mutation in the closely related P-glycoprotein *PGP1* did not confer resistance to the chemical, as *pgp1* mutants responded similarly as the wild-type when exposed to Gravacin (Figure 2). Similar to the *pgp19-1* (Figure 2) and *pgp19-4* (Figure 1B) mutants, the *pgp1 pgp19-1* double mutant was also resistant to Gravacin (Figure 2). These results together confirm that the mutation in *PGP19* of *pgp19-4* is responsible for its Gravacin-resistant phenotype.

It has been shown that the immunophilin-like TWISTED DWARF 1 (TWD1) protein interacts with both PGP19 and PGP1, and is required for their activity in planta [16]. Thus, several phenotypes observed in *pgp1 pgp19-1* double mutants are recapitulated in *twd1*. We then tested whether *twd1* mutants were resistant to Gravacin in the gravitropic assay, and indeed these seedlings were resistant to Gravacin as the *pgp19-1*, *pgp19-4*, and *pgp19 pgp1* double mutants (Figure 2), indicating that both *TWD1* and *PGP19* but not *PGP1* are required for the effect of Gravacin on gravitropism.

Effect of Gravacin on PGP-Mediated Auxin Transport

PGP19 was identified as a plasma membrane protein that binds the noncompetitive polar auxin transport inhibitor NPA [14, 15], and both *PGP19* and *PGP1* are required for auxin transport in shoots [15, 16]. Furthermore, PGP19 and PGP1 expressed in HeLa and tobacco-BY-2 cells are able to export auxin, and this activity is reduced by NPA [6, 7, 9]. Given the role of PGP19 in auxin transport, we wanted to determine the effect of the *pgp19-4* mutation and that of Gravacin in this process. Transport of radiolabeled auxin from the shoot apex to the shoot-root transition zone was used to measure shoot basipetal auxin transport in each genotype [16]. Basipetal auxin transport was significantly reduced in 5-day-old *pgp19-1*, *pgp1 pgp19*, double and *pin1* mutant seedlings when compared to wild-type as has previously been described [15, 16] (Figure 3A, black bars). Consistent with previous reports [15, 16] and under the conditions used, *pgp1* mutants showed only a slight decrease in auxin transport. Similar to *pgp19-1*, the *pgp19-4* allele exhibited a 50% reduction in basipetal auxin transport when compared to its parental control (GFP-δTIP in Col-0), indicating an important role of E1174 in the auxin transport activity of PGP19. To determine the effect of Gravacin in auxin transport, seedlings were exposed to 30 μM Gravacin for 2 hr prior to auxin transport measurements (Figure 3A, white bars). A 50% reduction in basipetal auxin transport was observed in wild-type Ws seedlings when treated with Gravacin. Treatment with lower concentrations of Gravacin or Gravacin treatments of shorter intervals resulted in lesser reductions in transport. However, when *pgp19-1*

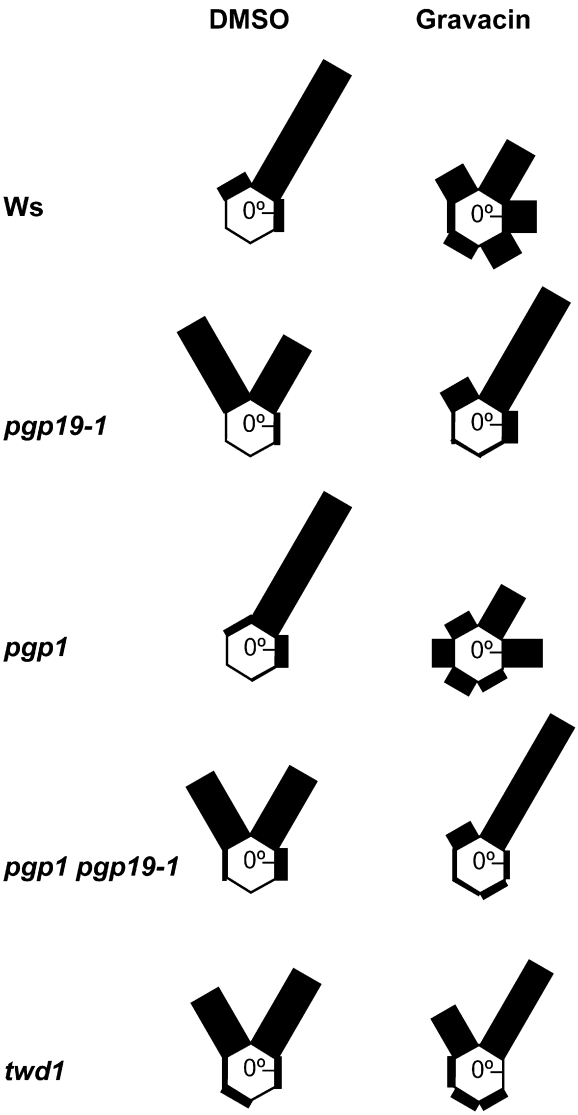

Figure 2. Mutations in *PGP19* Confer Resistance to Gravacin
Seeds from wild-type Ws, *pgp19-1*, *pgp1*, *pgp1 pgp19-1* double mutant, and *twd1* were tested in a gravitropic assay in the absence (left, DMSO) or presence (right) of 1 μM Gravacin. The gravitropic response was assayed as in Figure 1B, except that *twd1* data only include 30–40 seedlings per treatment.

or *pgp19-1 pgp1* double mutants were used, the reduction in transport due to the chemical was not significantly different from the untreated controls, indicating that PGP19 is required for the inhibition of auxin transport by Gravacin. When seedlings of *pin1* or *pgp1* mutants were assayed in the presence of Gravacin, the reduction in transport was between 30% and 50% of the corresponding untreated control. The GFP-δTIP line in the Col-0 background was also affected by Gravacin treatment; however, transport was reduced only by ~40%. Similar to *pgp19-1* and *pgp19-1 pgp1* double mutants, the basipetal auxin transport in hypocotyls of *pgp19-4* mutants was not affected by Gravacin treatment when compared to the

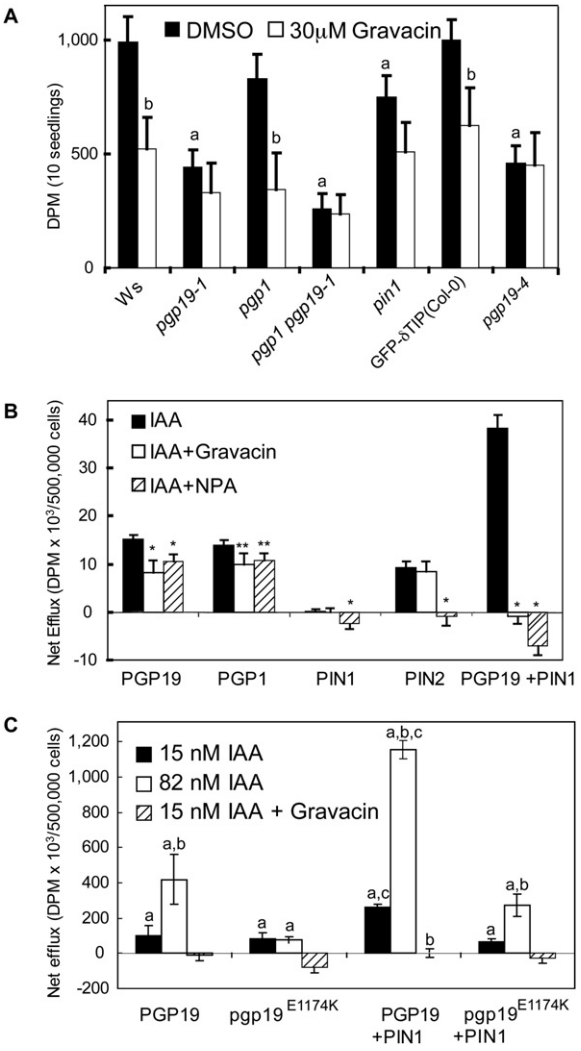

Figure 3. Gravacin Inhibits Auxin Transport
(A) The *pgp19-4* mutation and treatment with Gravacin have an effect on auxin transport in *Arabidopsis* shoots. Basipetal transport of [^{3}H]IAA in *Arabidopsis* hypocotyls from wild-type Ws, *pgp19-1*, *pgp1*, *pgp1 pgp19-1*, *pin1*, the parental line GFP-δTIP (ecotype Col-0), and *pgp19-4* in the presence of DMSO (black bars) or 30 μM Gravacin (white bars). Data represent mean ± SD (n = 10). Significant differences were determined by ANOVA followed by Tukey post-hoc analysis (a, different from corresponding wild-type control; b, different from the DMSO-treated value of the same genotype, $p < 0.05$).
(B) Effect of Gravacin on the auxin efflux activity of HeLa cells expressing PGP19, PGP1, PIN1, PIN2, or coexpressing PGP19 and PIN1 (PGP19 + PIN1). Cells were incubated with 25 nM [^{3}H]IAA alone (black bars), 25 nM [^{3}H]IAA and 5 μM Gravacin (white bars), or 25 nM [^{3}H]IAA and 5 μM NPA (crossed bars). Data represent mean ± SD. Significant differences between the IAA control and each treatment are indicated (ANOVA and Tukey post-hoc analysis: *$p < 0.01$, **$p < 0.1$).
(C) Effect of the E1174K substitution and Gravacin treatment on auxin efflux activity of PGP19 in HeLa cells. Net efflux of [^{3}H]IAA in HeLa cells expressing PGP19 or pgp19^{E1174K} proteins incubated with 15 nM (black bars) or 81.5 nM (white bars) [^{3}H]IAA alone, or 15 nM [^{3}H]IAA and 5 μM Gravacin (crossed bars). Data represent mean ± SD. Significant differences were determined by ANOVA and Tukey post-hoc analysis (a, different from the empty vector control; b, different from the corresponding 15 nM IAA treatment; c, coexpressed PGP19 + PIN1 (or pgp19^{E1174K} + PIN1 was different from the corresponding PGP19 alone, $p < 0.05$).

untreated control. These data together indicate that Gravacin inhibits basipetal auxin transport in wild-type hypocotyls via the inhibition of PGP19 activity.

The capacity of PIN2, PIN7, PGP1, and PGP19 to transport auxin independently in a heterologous system has been demonstrated [6, 7, 9, 20], and the synergistic interaction of PIN1 with PGP19 in the same system indicated that PIN-PGP interactions play a role in defining the specificity and rate of molecular transport [20]. We took advantage of this system to determine the effect of Gravacin on the efflux activity of individual transporters and coexpressed PGP19 and PIN1. PGP19, PGP1, PIN1, and PIN2 proteins were expressed in HeLa cells and the net efflux of radiolabeled auxin with and without 5 μM Gravacin or NPA was analyzed. As has been described previously, expression of PGP19, PGP1, and PIN2 results in significant net auxin efflux, but expression of PIN1 alone results in no detectable transport [6, 20] (Figure 3B). Similarly, coexpression of PGP19 and PIN1 resulted in a synergistic increase in auxin efflux [20]. Gravacin reduced the transport activity of PGP19 by 45% and that of PGP1 by almost 30%, but did not affect PIN2 transport. Auxin efflux was inhibited by Gravacin in cells expressing PGP19 + PIN1, which indicates that Gravacin may disrupt the interaction of PGP19 with other proteins. Concentrations of Gravacin higher than 5 μM (up to 30 μM) were not used because they increased IAA retention in all cells, decreased cell adhesion, and increased other visible symptoms of cellular toxicity. In contrast to Gravacin and consistent with previous results [9, 20], 5 μM NPA inhibited the auxin transport mediated by PIN2. NPA treatment also reduced the levels of auxin transport by PGP1, PGP19, and PIN1 + PGP19 to similar levels as Gravacin. Interestingly, 5 μM Gravacin has less of an effect on background HeLa cell transport activated by PIN1 expression [9, 20] than the same concentration of NPA, which highlights a higher specificity of Gravacin for PGP19. The effect of the E1174K substitution from *pgp19-4* was also tested in this system (Figure 3C). Expression of PGP19 harboring the mutation observed in *pgp19-4* (pgp19^{E1174K}) resulted in similar IAA efflux activity when cells were incubated with 15 nM [^{3}H]IAA. However, cells expressing pgp19^{E1174K} showed a 70% decrease in auxin transport compared to wild-type PGP19 when 81.5 nM [^{3}H]IAA was used (Figure 3C). This large difference was due in part to the increased transport activity of wild-type PGP19 at high auxin concentration, which was not observed in cells expressing pgp19^{E1174K}. This indicates that E1174 is important for the modulation of auxin efflux activity of PGP19 with varying concentrations of auxin. Coexpression of pgp19^{E1174K} with PIN1 did not result in the synergistic increase of transport that has been previously observed in cells coexpressing PGP19 and PIN1 both at 15 and 82 nM [^{3}H]IAA (Figure 3C), which points toward E1174 as an important residue involved in PGP19 interactions with PIN1. Treatment with 5 μM Gravacin resulted in inhibition of efflux activity in cells expressing PGP19, pgp19^{E1174K}, and pgp19^{E1174K} + PIN1. Experiments from Figure 3C were conducted using purified [^{3}H]IAA which results in increased loading into cells and increased the sensitivity of the assay.

Gravacin Binds PGP19 in *Arabidopsis* Microsomes

Microsomal fractions containing PGP19 have been shown to bind NPA with high affinity [14]. Thus, we asked whether Gravacin could compete with NPA for binding to *Arabidopsis* microsomes. Microsomes from wild-type Ws, *pgp19-1*, *pgp1*, and *pin1* mutants were incubated with 20 nM [^{3}H]NPA alone or [^{3}H]NPA and 100 nM Gravacin. To determine specific binding activity, the experiments were repeated in the presence of 20 μM cold NPA and residual binding was subtracted. Figure 4A shows that, when incubated with NPA alone (black bars), wild-type microsomes exhibit specific NPA binding of approximately 100 fmol [^{3}H]NPA/mg total protein in this assay. NPA binding was reduced in *pgp19-1* microsomes by about 50% when compared to wild-type, indicating that PGP19 is important for specific NPA binding to *Arabidopsis* microsomes. NPA binding did not significantly change in *pgp1* and *pin1* microsomes when compared to the wild-type control. When microsomes from wild-type Ws seedlings were incubated with both NPA and Gravacin (white bars), more than 60% of the NPA bound to microsomes was displaced by Gravacin. No significant displacement of [^{3}H]NPA by Gravacin was observed in microsomes isolated from *pgp19-1* seedlings, suggesting that [^{3}H]NPA bound to PGP19 is what is primarily displaced by Gravacin in the wild-type. This was further supported by results from the *pgp1* or *pin1* mutants which were very similar to the wild-type (Figure 4A).

To further ascertain whether PGP19 directly binds Gravacin and is responsible for its effect on seedling auxin transport, we assayed Gravacin binding to microsomal fractions from wild-type plants and from the two mutant alleles *pgp19-1* and *pgp19-4*. Microsomal fractions from each genotype were incubated with 15 μM Gravacin. Unbound Gravacin was removed by a series of washes in buffer lacking Gravacin, and bound chemical was measured by absorbance at 348 nm (Supplemental Data). Wild-type microsomes retained 40–47 pmol Gravacin/mg total protein (Figure 4B). Binding of Gravacin was significantly reduced in microsomes from *pgp19-1* and *pgp19-4* mutants compared to the corresponding controls wild-type Ws and GFP-δTIP, respectively. A significant decrease in Gravacin binding was also seen in *twd1*, indicating that TWD1 is involved, even if indirectly, in Gravacin binding to microsomes. Overall, these results are consistent with Gravacin binding to PGP19 and with the interpretation that the gravitropism resistance phenotype of *pgp19-4* hypocotyls is due to reduced binding of the chemical to the mutant pgp19^{E1174K} protein. However, the extent of Gravacin binding exceeds the apparent PGP19 protein content of wild-type microsomes as indicated by ELISAs (B.T., J.B., and A.S.M., unpublished data) and by NPA displacement experiments, suggesting that loss of PGP19 function impacts binding of Gravacin to other targets as well. This may be a result of the altered membrane characteristics previously observed in

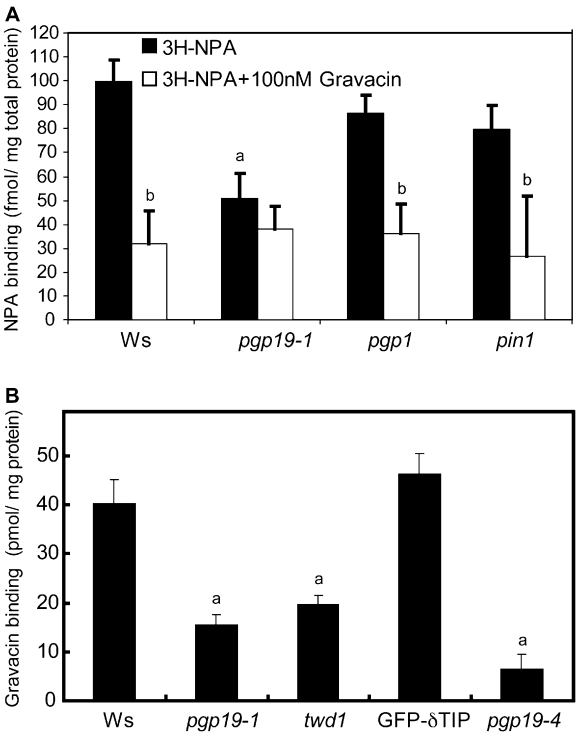

Figure 4. Gravacin Binds to Microsomes that Contain Active PGP19

(A) Gravacin displaces NPA from microsomes containing PGP19. [^{3}H]NPA binding was measured in microsomal fractions from Ws, *pgp19-1*, *pgp1*, or *pin1* that were incubated with 20 nM [^{3}H]NPA in the absence (black bars) or presence (white bars) of 100 nM Gravacin. Data represent means ± SD (n = 3). Significant differences from wild-type control (a) or from the NPA-alone value of the same genotype (b) are indicated (ANOVA and Tukey post-hoc analysis: $p < 0.001$).

(B) Gravacin binds to microsomes containing active PGP19. Binding of Gravacin to microsomal fractions from wild-type Ws, *pgp19-1*, *twd1*, the parental line GFP-δTIP, and *pgp19-4*. Gravacin was measured by absorbance at 348 nm. Data represent mean ± SD. Significant differences from wild-type control (a) are indicated (ANOVA and Tukey post-hoc analysis: $p < 0.001$).

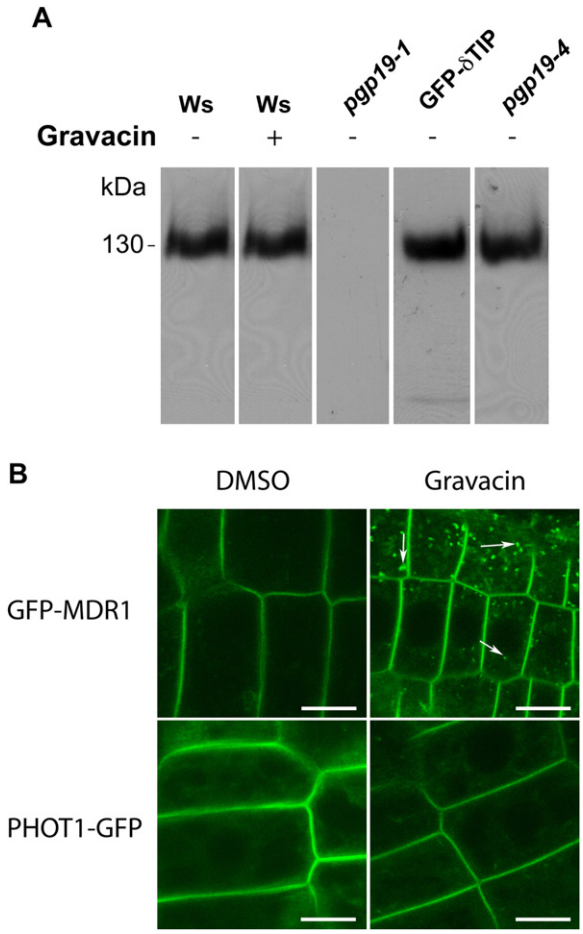

Figure 5. Effect of Gravacin on Protein Abundance and Localization

(A) Gravacin does not affect the abundance of PGP19. Equal amounts of microsomal membrane proteins from each genotype were analyzed by western blot using anti-PGP19 antibodies. Wild-type Ws seedlings were treated with DMSO or 5 μM Gravacin for 24 hr. The mutant alleles *pgp19-4* and *pgp19-1* as well as the GFP-δTIP control were not treated.

(B) Gravacin affects the subcellular localization of a PGP19 marker (GFP-MDR1). Three-day-old seedlings from the GFP-MDR1 (top) and PHOT1-GFP (bottom) marker lines were exposed to DMSO (left panel) or 5 μM Gravacin (right panel) for 48 hr before inspection of root tips under a confocal microscope. Bright punctate structures containing GFP-MDR1 that were induced by Gravacin treatment are indicated by arrows. The scale bars represent 10 μm.

pgp19-1 (B.T., J.B., and A.S.M., unpublished data). Furthermore, the saturating levels of Gravacin that were used for this assay may result in aggregation of Gravacin molecules at the plasma membrane as was previously described for NPA in similar experiments [40].

Gravacin Affects Localization of a GFP Fusion to PGP19

The effect of Gravacin on the auxin transport activity of PGP19 may be due to effects in abnormal protein abundance or localization, or direct inhibition of protein activity at the plasma membrane. Treatment of wild-type Ws seedlings with 5 μM Gravacin for 24 hr did not affect the overall abundance of PGP19 in microsomal fractions (Figure 5A). In contrast to the *pgp19-1* knockout [15], the *pgp19-4* line accumulates mutant protein at similar levels as the wild-type (Figure 5A), indicating that this mutation does not affect protein stability. We then used a GFP fusion to PGP19 (GFP-MDR1) [18] as well as a marker for another plasma membrane protein, PHOT1-GFP [41], to determine the effect of Gravacin on their localization. Similarly to the control, 48 hr of 5 μM Gravacin treatment resulted in accumulation of GFP-MDR1 fusion protein in the plasma membrane. However, the fusion protein also accumulated in an unidentified endomembrane compartment that was not labeled in the control (Figure 5B). Lack of colocalization with the endocytic marker FM4-64 indicated that this punctate compartment is not endosome (Figure S3). Thus, this abnormal localization is most likely due to an abnormal delivery of this marker to the plasma membrane. In comparison with the GFP-MDR1 marker,

no differences in the localization of PHOT1-GFP were observed in Gravacin-treated seedlings (Figure 5B).

We have shown that PGP19 is not the target responsible for the effect of Gravacin on trafficking of the GFP-δTIP marker (Table 1). As expected, *pgp19-4* mutants have wild-type sensitivity to the effect of Gravacin on the trafficking of the tonoplast protein marker GFP-δTIP (Figure S4). This indicates that *pgp19-4* is not resistant to the effect of Gravacin on protein trafficking, and further corroborates the finding that a target other than PGP19 is implicated in this phenotype of Gravacin-treated seedlings.

DISCUSSION

We provided several lines of evidence to demonstrate that PGP19 is an important target of Gravacin, and that PGP19, together with another target(s), participates in the agravitropic phenotype of seedlings grown in this chemical. First, we showed that the inhibition of basipetal auxin transport by Gravacin in wild-type *Arabidopsis* hypocotyls requires PGP19. Therefore, mutations in *PGP19* confer resistance to Gravacin, both in terms of its effect on gravitropism and inhibition of basipetal auxin transport, and this is not due to abnormal uptake or metabolism of the chemical inside plant cells. The phenotype of four alleles confirmed that the lesions in the *PGP19* locus are responsible for the Gravacin-resistant phenotypes of these mutants. Direct inhibition of PGP19 by Gravacin was demonstrated when Gravacin significantly inhibited the efflux activity of PGP19 and PGP19 + PIN1 proteins expressed in HeLa cells. Also, NPA has been shown to bind plasma membrane fractions containing PGP19 [14] and yeast cells expressing PGP19 can bind NPA [15], indicating that PGP19 is one target of NPA. We showed here that PGP19 is required for Gravacin competition with NPA for binding sites, as Gravacin was able to displace NPA from NPA binding sites only in microsomes that contained PGP19. Finally, Gravacin binds to *Arabidopsis* microsomes from wild-type plants, but a single amino acid change in the PGP19 protein reduced Gravacin binding to microsomes from *pgp19-4* mutants to levels below the linear detection limits of the assay. The knockout allele *pgp19-1* also exhibited reduced binding of chemical to microsomes, but it was less severe than the *pgp19-4* allele. This mutant has been shown to upregulate other PGP proteins to compensate for the absence of PGP19 [20] and thus the Gravacin chemical is likely to bind to other PGP proteins as well.

We have shown that Gravacin inhibits the auxin transport activity of light-grown *Arabidopsis* hypocotyls to levels similar to those seen in the *pgp19-1* null allele. In the dark, the loss of PGP19 function in the *pgp19-1* mutant results in the hypertropic bending phenotype as a result of reduced basipetal auxin transport [34], and this phenotype is less severe in the *pgp19-4* allele. However, although Gravacin treatment resulted in completely agravitropic growth in the wild-type, both *pgp19-1* and *pgp19-4* exhibited Gravacin resistance as gravitropic bending was only slightly inhibited. This indicated that PGP19 is *required* for the agravitropic phenotype of Gravacin-treated seedlings and led us to the following conclusions: (1) PGP19 is likely only one of several targets of Gravacin that mediate gravitropism. Thus, Gravacin interactions with other cellular components may be necessary to prevent graviperception in wild-type seedlings. (2) Gravacin is likely to affect PGP19 interactions with other proteins, as Gravacin had the greatest impact on auxin transport in HeLa cells coexpressing PIN1 and PGP19. Furthermore, the *pgp19-4* mutation, which abolished Gravacin binding to PGP19, is located in the C-terminal tail previously shown to mediate interactions with both TWD1 and PIN [16, 20]. Thus, although Gravacin affects PGP19 interactions in wild-type, basal transport of these PGP19-interacting proteins, if not affected by Gravacin, may be sufficient for generating the gradients necessary for hypocotyl bending in *pgp19* mutants when exposed to this chemical. (3) Compensatory increased expression of *PIN*s and *PGP*s seen in the *pgp19-1* [20] may provide sufficient basal auxin movement in Gravacin-treated *pgp19-1* seedlings to restore gravitropism.

Our results together imply that the second nucleotide binding domain of PGP19 and specifically E1174 are important for the auxin transport activity of PGP19, both in plants and in the HeLa cell system, its interaction with PIN1, and its ability to bind Gravacin. Hence, the E1174K substitution in the second nucleotide binding domain of PGP19 may be sufficient for a structural change in the loop of PGP19 that binds Gravacin and changes its affinity for this compound. E1174 is the next residue following the predicted Walker B box (VLLLD) as part of the nucleotide binding fold of this protein. This residue is highly conserved among ABC transporters from several organisms and has been shown to bind water and an Mg^{2+} ion as part of the ATP hydrolysis mechanism of these proteins. Thus, mutations in this glutamate render other ABC transporters inactive for ATP hydrolysis [42, 43].

The resistant phenotype of gravistimulated *twd1* seedlings and reduced microsomal binding of these mutants to Gravacin raises the question of whether TWD1 is also a target of Gravacin. However, TWD1 regulates both PGP19 and PGP1 such that if TWD1 were a target of Gravacin, then *pgp1* mutants should display a resistant phenotype similar to that of *pgp19* mutants. As *pgp1* mutants exhibit agravitropic phenotypes in the presence of Gravacin and Gravacin does not phenocopy the twisting phenotype of the *twd1* mutant [16], we conclude that TWD1 is probably not a target of Gravacin. TWD1 interacts with the C-terminal domains of PGP19 and PGP1, and is required for PGP19 and PGP1 activity in planta [6, 16]. Yeast two-hybrid analysis indicates that the *cis-trans* peptidylprolyl isomerase (PPIase) domain of TWD1 interacts with the C-terminal domain of PGP19 (amino acids 965–1252) [16] that harbors the *pgp19-4* mutation. The Gravacin-resistant phenotype of *twd1* is consistent with the model proposed by Bouchard et al. [6], whereby TWD1 is required for conformational changes that would result in ATP access to the second nucleotide binding domain of PGP1 and PGP19. This phenotype suggests that

binding to PGP19 is reduced in these mutants because it is conformationally biased toward the inactive state. We speculate that Gravacin binding to wild-type PGP19 occurs primarily in the state activated by TWD1, as Gravacin-binding activity of *twd1* microsomes is only about 60% of that of the wild-type.

Gravacin is a more specific tool for dissecting auxin transport mechanisms because, unlike NPA, it does not appear to affect PIN proteins and did not induce the background activity of transporters in HeLa cells. Gravacin may inhibit the activity of PGP19 in part by affecting its localization, probably via reduced delivery to the plasma membrane as was shown for the GFP-MDR1 marker. That Gravacin-induced punctate bodies containing GFP-MDR1 were not endosomal correlated well with previous evidence that PGP19 does not appear to be regulated by endocytic cycling at the plasma membrane [20]. However, direct inhibition of PGP19 at the plasma membrane is also likely given the amount of GFP-MDR1 fusion protein that was present at the plasma membrane after chemical treatment. We speculate that the interaction of PGP19 with Gravacin may occur at the nucleotide binding domains because of the reduced binding of Gravacin to microsomes from the *pgp19-4* mutant which produces the E1174K substitution in the second nucleotide binding domain of this protein. Also, few changes in the Gravacin molecule were sufficient for the loss of the gravitropic inhibition, which suggests a close relationship between PGP19 and the Gravacin molecule.

The target responsible for the effect of Gravacin on GFP-δTIP trafficking is still unknown, but its interaction with Gravacin occurs in a different time frame. Thus, although at least 48 hr of treatment is required in seedlings to induce this phenotype (not shown), a 2 hr treatment was sufficient to induce changes in the transport activity of PGP19.

SIGNIFICANCE

PGP19 is 38% identical overall and 54% identical at the C-terminal nucleotide binding domain to the human PGP-MDR1 (HsP-gp), the best-studied ABC transporter involved in multidrug resistance of tumor cells. Overexpression of HsP-gp in cancer cells results in exclusion of cytotoxic drugs during treatment, and inhibitors of HsP-gp are being analyzed for their potential in cancer therapy [44]. The nucleotide binding domains have been identified as a potent target for P-gp inhibition given their crucial role for transport activity [44]. The effect of Gravacin on localization and activity of PGP19 can be potentially useful for the development of inhibitors of HsP-gp for cancer treatment with large implications for human health.

EXPERIMENTAL PROCEDURES

Plant Materials and Growth Conditions

The 35S:GFP-δTIP line [45] is in the Columbia (Col-0) ecotype and was previously mutagenized by ethylmethane sulfonate (EMS) [37]. *pgp19-1*, *pgp1*, *pgp19 pgp1*, and *twd1* [15] mutants are in the Wassilewskija (Ws) ecotype. *mdr1-100* and *mdr1-101* [39] are in the Col-0 ecotype and were a gift from Haiyang Wang (Cornell University). The GFP-MDR1 [18] and PHOT1-GFP [41] fusion markers were gifts from Edgar Spalding (University of Wisconsin) and Winslow Briggs (Carnegie Institution of Washington), respectively. Wild-type Col-0 and Ws were originally obtained from the *Arabidopsis* Biological Resource Center. All plants were grown under long-day conditions (16/8 hr photoperiod) at 22°C under cool fluorescent lights (photosynthetic photon flux density of 120 $\mu M\ m^{-1}\ s^{-1}$). Sterile seeds were plated on 0.5× Murashige and Skoog [46] agar media supplemented with either chemical or a corresponding amount of DMSO ($\leq$0.1%). One percent sucrose was used in the media except for the experiments with analogs which were done in media without sucrose.

Chemical-Induced Phenotypes in Seedlings and Mutant Screen

For gravitropic assays, plates were incubated in the dark at 4°C for 2 days and then exposed to light for 14 hr at 22°C. Plates were wrapped in foil and incubated in vertical orientation for 3 days, turned 90°, and scored 24 hr later. For the resistant mutant screen, seeds were plated on large square plates containing growth media supplemented with 1.7 μM Gravacin and arranged individually 1–2 cm apart. Seven hundred and eight putative resistant seedlings that responded correctly to gravitropic stimulus were transplanted to soil, but only 350 plants set viable seeds. A secondary screen yielded only 7 resistant mutants. Hypocotyl curvatures after 24 hr gravistimulation were measured using ImageJ (National Institutes of Health) [36].

For protein abundance, seeds were plated in vertical mesh transfer boxes [47]. Five-day-old seedlings were sprayed with 5 μM Gravacin and incubated for 24 hr. Microsomes were prepared as described [14] with the exception that 0.2% (v/v) β-methyl cyclodextrin was added to the final resuspension buffer, followed by an incubation on ice for 30 min. Samples were incubated at 37°C for 30 min prior to SDS-PAGE (8% gels) and immunoblot analysis. The immunoblot was probed with anti-PGP19 [20] at a dilution of 1:2500, followed by anti-rabbit IgG-horseradish peroxidase-conjugated secondary antibody at a dilution of 1:3000 (Amersham Biosciences, Piscataway, NJ, USA) and detected by enhanced chemiluminescent reagents (Amersham Bioscience).

Chemicals Used

These chemicals were obtained from ChemBridge (San Diego, CA, USA): Gravacin (ID 5850247), compounds A (ID 5123159), B (ID 5860541), and C (ID 5878151). Compounds D (Aldrich, St. Louis, MO, USA; F20807-25G), E (Aldrich, 574112-5G), F (Ambinter, Paris, France; STOCK3S-96809), and G (Aldrich, 592773-5G) were obtained as indicated. Chemicals were dissolved in 100% DMSO as 35 mM stocks.

Gene Mapping

Segregating F_2-resistant plants were isolated using the gravitropic assay. DNA from individual plants was isolated with Trizol reagent (Invitrogen, Carlsbad, CA, USA), and SSLP markers [38] were used for rough mapping.

Confocal Microscopy

Seedling roots from GFP markers were analyzed under a Leica TCS SP2 laser-scanning confocal microscope (Leica, Wetzlar, Germany).

Auxin Transport Measurements

Basipetal auxin transport in hypocotyls was measured as previously described [16]. All statistical analyses were done with SigmaStat (Jandel Scientific, Cupertino, CA, USA).

NPA and Gravacin Binding Assays

Plasma membrane-enriched microsomes from each genotype were incubated with 0.62 mCi (20 nM) [^{3}H]NPA (specific activity 31 Ci/mmol;

American Radiolabeled Chemicals, St. Louis, MO, USA). NPA binding was estimated as described [15], but the assay was performed in the presence of DMSO or 100 nM Gravacin. For Gravacin binding, purified microsomes were incubated for 30 min on ice with 15 μM Gravacin and collected by centrifugation at 100,000 × g. After two additional resuspensions in 500 μl of buffer lacking Gravacin and subsequent recentrifugation, the concentration of chemical that remained in the microsomal pellets was estimated by absorbance at 348 nm. A standard curve was generated for each wild-type control by measuring absorbance at 348 nm of solutions containing different concentrations of Gravacin and aliquots of microsomes that had been washed three times as described above.

HeLa Assays

Constructs of PGP19, PGP1, PIN1, and PIN2 in the pTM1 vector [48] for expression in HeLa cells have been described [6, 9, 20]. For expression of the pgp19^{E1174K} protein, the pTM1 construct containing the PGP19-HA cDNA fusion was site-specific mutagenized using the Quikchange II XL site-directed mutagenesis kit (Stratagene, La Jolla, CA, USA). The [^{3}H]IAA transport assays were performed as previously described [7], except that 5 μM Gravacin or 5 μM NPA was added to the transfected/infected HeLa cells and incubated for 2 hr prior to the assay.

Supplemental Data

Supplemental Data include four figures and Supplemental Experimental Procedures and can be found with this article online at http://www.chembiol.com/cgi/content/full/14/12/1366/DC1/.

ACKNOWLEDGMENTS

We thank members of the Raikhel laboratory for useful discussions and critical reading of the manuscript. We thank H. Wang (Cornell University) for providing *mdr1-100* and *mdr1-101* seeds and E. Spalding (University of Wisconsin) for providing the GFP-MDR1 line. This work was supported by National Science Foundation grant MCB-0520325 to N.V.R.

Received: July 5, 2007
Revised: September 24, 2007
Accepted: October 22, 2007
Published: December 26, 2007

REFERENCES

1. Higgins, C.F. (1992). ABC transporters: from microorganisms to man. Annu. Rev. Cell Biol. *8*, 67–113.
2. Borst, P., and Elferink, R.O. (2002). Mammalian ABC transporters in health and disease. Annu. Rev. Biochem. *71*, 537–592.
3. Rea, P.A. (2007). Plant ATP-binding cassette transporters. Annu. Rev. Plant Biol. *58*, 347–375.
4. Geisler, M., and Murphy, A.S. (2006). The ABC of auxin transport: the role of p-glycoproteins in plant development. FEBS Lett. *580*, 1094–1102.
5. Sanchez-Fernandez, R., Davies, T.G., Coleman, J.O., and Rea, P.A. (2001). The *Arabidopsis thaliana* ABC protein superfamily, a complete inventory. J. Biol. Chem. *276*, 30231–30244.
6. Bouchard, R., Bailly, A., Blakeslee, J.J., Oehring, S.C., Vincenzetti, V., Lee, O.R., Paponov, I., Palme, K., Mancuso, S., Murphy, A.S., et al. (2006). Immunophilin-like TWISTED DWARF1 modulates auxin efflux activities of *Arabidopsis* P-glycoproteins. J. Biol. Chem. *281*, 30603–30612.
7. Geisler, M., Blakeslee, J.J., Bouchard, R., Lee, O.R., Vincenzetti, V., Bandyopadhyay, A., Titapiwatanakun, B., Peer, W.A., Bailly, A., Richards, E.L., et al. (2005). Cellular efflux of auxin catalyzed by the *Arabidopsis* MDR/PGP transporter AtPGP1. Plant J. *44*, 179–194.
8. Terasaka, K., Blakeslee, J.J., Titapiwatanakun, B., Peer, W.A., Bandyopadhyay, A., Makam, S.N., Lee, O.R., Richards, E.L., Murphy, A.S., Sato, F., et al. (2005). PGP4, an ATP binding cassette P-glycoprotein, catalyzes auxin transport in *Arabidopsis thaliana* roots. Plant Cell *17*, 2922–2939.
9. Petrasek, J., Mravec, J., Bouchard, R., Blakeslee, J.J., Abas, M., Seifertova, D., Wisniewska, J., Tadele, Z., Kubes, M., Covanova, M., et al. (2006). PIN proteins perform a rate-limiting function in cellular auxin efflux. Science *312*, 914–918.
10. Galweiler, L., Guan, C., Muller, A., Wisman, E., Mendgen, K., Yephremov, A., and Palme, K. (1998). Regulation of polar auxin transport by AtPIN1 in *Arabidopsis* vascular tissue. Science *282*, 2226–2230.
11. Paponov, I.A., Teale, W.D., Trebar, M., Blilou, I., and Palme, K. (2005). The PIN auxin efflux facilitators: evolutionary and functional perspectives. Trends Plant Sci. *10*, 170–177.
12. Friml, J., and Palme, K. (2002). Polar auxin transport—old questions and new concepts? Plant Mol. Biol. *49*, 273–284.
13. Muller, A., Guan, C., Galweiler, L., Tanzler, P., Huijser, P., Marchant, A., Parry, G., Bennett, M., Wisman, E., and Palme, K. (1998). AtPIN2 defines a locus of *Arabidopsis* for root gravitropism control. EMBO J. *17*, 6903–6911.
14. Murphy, A.S., Hoogner, K.R., Peer, W.A., and Taiz, L. (2002). Identification, purification, and molecular cloning of N-1-naphthylphthalmic acid-binding plasma membrane-associated aminopeptidases from *Arabidopsis*. Plant Physiol. *128*, 935–950.
15. Noh, B., Murphy, A.S., and Spalding, E.P. (2001). Multidrug resistance-like genes of *Arabidopsis* required for auxin transport and auxin-mediated development. Plant Cell *13*, 2441–2454.
16. Geisler, M., Kolukisaoglu, H.U., Bouchard, R., Billion, K., Berger, J., Saal, B., Frangne, N., Koncz-Kalman, Z., Koncz, C., Dudler, R., et al. (2003). TWISTED DWARF1, a unique plasma membrane-anchored immunophilin-like protein, interacts with *Arabidopsis* multidrug resistance-like transporters AtPGP1 and AtPGP19. Mol. Biol. Cell *14*, 4238–4249.
17. Geisler, M., Girin, M., Brandt, S., Vincenzetti, V., Plaza, S., Paris, N., Kobae, Y., Maeshima, M., Billion, K., Kolukisaoglu, U.H., et al. (2004). *Arabidopsis* immunophilin-like TWD1 functionally interacts with vacuolar ABC transporters. Mol. Biol. Cell *15*, 3393–3405.
18. Wu, G., Lewis, D.R., and Spalding, E.P. (2007). Mutations in *Arabidopsis* multidrug resistance-like ABC transporters separate the roles of acropetal and basipetal auxin transport in lateral root development. Plant Cell *19*, 1826–1837.
19. Lewis, D.R., Miller, N.D., Splitt, B.L., Wu, G., and Spalding, E.P. (2007). Separating the roles of acropetal and basipetal auxin transport on gravitropism with mutations in two *Arabidopsis* multidrug resistance-like ABC transporter genes. Plant Cell *19*, 1838–1850.
20. Blakeslee, J.J., Bandyopadhyay, A., Lee, O.R., Mravec, J., Titapiwatanakun, B., Sauer, M., Makam, S.N., Cheng, Y., Bouchard, R., Adamec, J., et al. (2007). Interactions among PIN-FORMED and P-glycoprotein auxin transporters in *Arabidopsis*. Plant Cell *19*, 131–147.
21. Blakeslee, J.J., Peer, W.A., and Murphy, A.S. (2005). Auxin transport. Curr. Opin. Plant Biol. *8*, 494–500.
22. Terasaka, K., Murphy, A.S., Sato, F., and Yazaki, K. (2005). Gene expression and functional analyses of a P-glycoprotein-like (PGP) ABC protein gene, AtPGP4, in *Arabidopsis thaliana*. Plant Cell Physiol. *46*, S35.
23. Swarup, R., Kargul, J., Marchant, A., Zadik, D., Rahman, A., Mills, R., Yemm, A., May, S., Williams, L., Millner, P., et al. (2004). Structure-function analysis of the presumptive *Arabidopsis* auxin permease AUX1. Plant Cell *16*, 3069–3083.

24. Swarup, R., Kramer, E.M., Perry, P., Knox, K., Leyser, H.M., Haseloff, J., Beemster, G.T., Bhalerao, R., and Bennett, M.J. (2005). Root gravitropism requires lateral root cap and epidermal cells for transport and response to a mobile auxin signal. Nat. Cell Biol. *7*, 1057–1065.

25. Blancaflor, E.B., and Masson, P.H. (2003). Plant gravitropism. Unraveling the ups and downs of a complex process. Plant Physiol. *133*, 1677–1690.

26. Ottenschlager, I., Wolff, P., Wolverton, C., Bhalerao, R.P., Sandberg, G., Ishikawa, H., Evans, M., and Palme, K. (2003). Gravity-regulated differential auxin transport from columella to lateral root cap cells. Proc. Natl. Acad. Sci. USA *100*, 2987–2991.

27. Boonsirichai, K., Sedbrook, J.C., Chen, R., Gilroy, S., and Masson, P.H. (2003). ALTERED RESPONSE TO GRAVITY is a peripheral membrane protein that modulates gravity-induced cytoplasmic alkalinization and lateral auxin transport in plant statocytes. Plant Cell *15*, 2612–2625.

28. Li, Y., Hagen, G., and Guilfoyle, T.J. (1991). An auxin-responsive promoter is differentially induced by auxin gradients during tropisms. Plant Cell *3*, 1167–1175.

29. Muday, G.K. (2001). Auxins and tropisms. J. Plant Growth Regul. *20*, 226–243.

30. Li, J., Yang, H., Peer, W.A., Richter, G., Blakeslee, J., Bandyopadhyay, A., Titapiwantakun, B., Undurraga, S., Khodakovskaya, M., Richards, E.L., et al. (2005). *Arabidopsis* H^+-PPase AVP1 regulates auxin-mediated organ development. Science *310*, 121–125.

31. Abas, L., Benjamins, R., Malenica, N., Paciorek, T., Wisniewska, J., Moulinier-Anzola, J.C., Sieberer, T., Friml, J., and Luschnig, C. (2006). Intracellular trafficking and proteolysis of the *Arabidopsis* auxin-efflux facilitator PIN2 are involved in root gravitropism. Nat. Cell Biol. *8*, 249–256.

32. Vieten, A., Sauer, M., Brewer, P.B., and Friml, J. (2007). Molecular and cellular aspects of auxin-transport-mediated development. Trends Plant Sci. *12*, 160–168.

33. Friml, J., Wisniewska, J., Benkova, E., Mendgen, K., and Palme, K. (2002). Lateral relocation of auxin efflux regulator PIN3 mediates tropism in *Arabidopsis*. Nature *415*, 806–809.

34. Noh, B., Bandyopadhyay, A., Peer, W.A., Spalding, E.P., and Murphy, A.S. (2003). Enhanced gravi- and phototropism in plant mdr mutants mislocalizing the auxin efflux protein PIN1. Nature *423*, 999–1002.

35. Blakeslee, J.J., Bandyopadhyay, A., Peer, W.A., Makam, S.N., and Murphy, A.S. (2004). Relocalization of the PIN1 auxin efflux facilitator plays a role in phototropic responses. Plant Physiol. *134*, 28–31.

36. Surpin, M., Rojas-Pierce, M., Carter, C., Hicks, G.R., Vasquez, J., and Raikhel, N.V. (2005). The power of chemical genomics to study the link between endomembrane system components and the gravitropic response. Proc. Natl. Acad. Sci. USA *102*, 4902–4907.

37. Avila, E.L., Zouhar, J., Agee, A.E., Carter, D.G., Chary, S.N., and Raikhel, N.V. (2003). Tools to study plant organelle biogenesis. Point mutation lines with disrupted vacuoles and high-speed confocal screening of green fluorescent protein-tagged organelles. Plant Physiol. *133*, 1673–1676.

38. Lukowitz, W., Gillmor, C.S., and Scheible, W.-R. (2000). Positional cloning in *Arabidopsis*. Why it feels good to have a genome initiative working for you. Plant Physiol. *123*, 795–805.

39. Lin, R., and Wang, H. (2005). Two homologous ATP-binding cassette transporter proteins, AtMDR1 and AtPGP1, regulate *Arabidopsis* photomorphogenesis and root development by mediating polar auxin transport. Plant Physiol. *138*, 949–964.

40. Murphy, A., and Taiz, L. (1999). Naphthylphthalamic acid is enzymatically hydrolyzed at the hypocotyl-root transition zone and other tissues of *Arabidopsis thaliana* seedlings. Plant Physiol. Biochem. *37*, 413–430.

41. Sakamoto, K., and Briggs, W.R. (2002). Cellular and subcellular localization of phototropin 1. Plant Cell *14*, 1723–1735.

42. Davidson, A.L., and Chen, J. (2004). ATP-binding cassette transporters in bacteria. Annu. Rev. Biochem. *73*, 241–268.

43. Smith, P.C., Karpowich, N., Millen, L., Moody, J.E., Rosen, J., Thomas, P.J., and Hunt, J.F. (2002). ATP binding to the motor domain from an ABC transporter drives formation of a nucleotide sandwich dimer. Mol. Cell *10*, 139–149.

44. McDevitt, C.A., and Callaghan, R. (2007). How can we best use structural information on P-glycoprotein to design inhibitors? Pharmacol. Ther. *113*, 429–441.

45. Cutler, S.R., Ehrhardt, D.W., Griffitts, J.S., and Somerville, C.R. (2000). Random GFP: cDNA fusions enable visualization of subcellular structures in cells of *Arabidopsis* at a high frequency. Proc. Natl. Acad. Sci. USA *97*, 3718–3723.

46. Murashige, T., and Skoog, F. (1962). A revised medium for rapid growth and bio assays with tobacco tissue cultures. Physiol. Plant. *15*, 473–497.

47. Murphy, A., and Taiz, L. (1995). A new vertical mesh transfer technique for metal-tolerance studies in *Arabidopsis* (ecotypic variation and copper-sensitive mutants). Plant Physiol. *108*, 29–38.

48. Hrycyna, C.A., Ramachandra, M., Pastan, I., and Gottesman, M.M. (1998). Functional expression of human P-glycoprotein from plasmids using vaccinia virus-bacteriophage T7 RNA polymerase system. Methods Enzymol. *292*, 456–473.

